with developmental defects.[5–14] Indeed, previous studies have shown that terminal duplications of 4q result in various clinical abnormalities, including mental retardation, short stature, microcephaly, facial dysmorphism and finger anomalies.[5,6] Of these, mental retardation is likely to be associated with copy-number gain of *GLRA3* or *GPM6A*,[7,8] whereas craniofacial features and minor limb abnormalities can be ascribed to *HAND2* duplication.[9] Terminal deletions of 7q are known to cause haploinsufficiency of *SHH* that leads to holoprosencephaly, mental retardation, single incisor and limb anomalies.[10] This 7q35-36 region also harbors several genes such as *CNTNAP2*, *EZH2*, *KCNH2* and *PRKAG2*, whose haploinsufficiency has been associated with congenital malformations and/or neurological abnormalities.[11–14] In contrast, the pathogenicity of the relatively small duplication on Xp22.3 remains unclear; Li *et al.*[15] reported that CNVs at Xp22.3 are shared by 0.37% of individuals with neuropsychological disabilities and/or congenital anomalies and by 0.15% of healthy controls. Taken together, the mental retardation and mild brain anomalies, and probably skeletal deformities as well, of our patient are ascribable to one or more of these three CNVs. As molecular analysis was not performed for patient's relatives except for the mother, it remains unknown whether these CNVs underlie mental retardation in his sisters and uncles. Furthermore, endocrinological evaluation was not performed for the patient's mother with the same Xp22.3 duplication, and therefore the association between the CNV and hormonal abnormalities remained unknown. Although the boy lacked most of the characteristic features of 4q terminal duplications and 7q terminal deletions, this can be explained by a relatively incomplete penetrance or variable expressivity of these features.[7,10] In particular, the lack of holoprosencephaly in this patient is consistent with the broad phenotypic spectrum of *SHH* haploinsufficiency.[16] Alternatively, this patient may have somatic mosaicism.

The patient manifested additional clinical features that have not been reported in patients with 4q duplications, 7q deletions or Xp22.3 duplications. The most remarkable findings were central precocious puberty and mild ACTH overproduction. The origin of elevated ACTH levels in this case has yet to be studied. The hormone data are indicative of ACTH resistance; however, the patient showed no signs of glucocorticoid deficiency characteristic of ACTH resistance.[17] Furthermore, it remains unclear whether precocious puberty and ACTH overproduction are independent events. Precocious puberty has not been described in patients with ACTH overproduction due to *MC2R* or *MRAP* mutations,[17] although ACTH-dependent precocious pseudopuberty was observed in an infant with adrenal hypoplasia due to *DAX1* mutations,[18] and ACTH is known to stimulate testosterone production in the neonatal mouse testis.[19] The CNVs in our patient included no known genes involved in the regulation of pituitary or adrenal hormones. However, since central precocious puberty and ACTH overproduction are genetically heterogeneous conditions,[17,20] hitherto unidentified causative genes may reside within these CNVs. Further studies are necessary to clarify the etiology of the unique phenotype of the patient.

In summary, we identified a boy with three cryptic CNVs. The boy manifested mental retardation, mild brain anomalies and skeletal deformities that are ascribable to the CNVs on 4q, 7q and/or Xp, together with endocrine abnormalities of unknown genetic origin.

HGV DATABASE

The relevant data from this Data Report are hosted at the Human Genome Variation Database at http://dx.doi.org/10.6084/m9.figshare.hgv.592, http://dx.doi.org/10.6084/m9.figshare.hgv.594, http://dx.doi.org/10.6084/m9.figshare.hgv.596.

ACKNOWLEDGEMENTS

This work was supported by the Grants-in-Aid from the Ministry of Education, Culture, Sports, Science and Technology, from the Japan Society for the Promotion of Science and by the Grants from the Ministry of Health, Labor and Welfare, from National Center for Child Health and Development and from Takeda foundation.

COMPETING INTERESTS

The authors declare no conflict of interest.

REFERENCES

1 Di Gregorio E, Savin E, Biamino E, Belligni EF, Naretto VG, D'Alessandro G *et al.* Large cryptic genomic rearrangements with apparently normal karyotypes detected by array-CGH. *Mol Cytogenet* 2014; **7**: 82.
2 Lee C, Iafrate AJ, Brothman AR. Copy number variations and clinical cytogenetic diagnosis of constitutional disorders. *Nat Genet* 2007; **39**: S48–S54.
3 Miller DT, Adam MP, Aradhya S, Biesecker LG, Brothman AR, Carter NP *et al.* Consensus statement: chromosomal microarray is a first-tier clinical diagnostic test for individuals with developmental disabilities or congenital anomalies. *Am J Hum Genet* 2010; **86**: 749–764.
4 Isojima T, Shimatsu A, Yokoya S, Chihara K, Tanaka T, Hizuka N *et al.* Standardized centile curves and reference intervals of serum insulin-like growth factor-I (IGF-I) levels in a normal Japanese population using the LMS method. *Endocr J* 2012; **59**: 771–780.
5 Mikelsaar RV, Lurie IW, Ilus TE. "Pure" partial trisomy 4q25-qter owing to a de novo 4;22 translocation. *J Med Genet* 1996; **33**: 344–345.
6 Egritas O, Cavdarli B, Dalgic B, Ergun MA, Percin F, Ziegler M *et al.* Duplication 4q associated with chronic cholestatic changes in liver biopsy. *Eur J Med Genet* 2010; **53**: 411–414.
7 Thapa M, Asamoah A, Gowans GC, Platky KC, Barch MJ, Mouchrani P *et al.* Molecular characterization of distal 4q duplication in two patients using oligonucleotide array-based comparative genomic hybridization (oaCGH) analysis. *Am J Med Genet A* 2014; **164A**: 1069–1074.
8 Gregor A, Kramer JM, van der Voet M, Schanze I, Uebe S, Donders R *et al.* Altered GPM6A/M6 dosage impairs cognition and causes phenotypes responsive to cholesterol in human and drosophila. *Hum Mutat* 2014; **35**: 1495–1505.
9 Tamura M, Hosoya M, Fujita M, Iida T, Amano T, Maeno A *et al.* Overdosage of Hand2 causes limb and heart defects in the human chromosomal disorder partial trisomy distal 4q. *Hum Mol Genet* 2013; **22**: 2471–2481.
10 Frints SG, Schoenmakers EF, Smeets E, Petit P, Fryns JP. De novo 7q36 deletion: breakpoint analysis and types of holoprosencephaly. *Am J Med Genet* 1998; **75**: 153–158.
11 Mikhail FM, Lose EJ, Robin NH, Descartes MD, Rutledge KD, Rutledge SL *et al.* Clinically relevant single gene or intragenic deletions encompassing critical neurodevelopmental genes in patients with developmental delay, mental retardation, and/or autism spectrum disorders. *Am J Med Genet A* 2011; **155A**: 2386–2396.
12 Tatton-Brown K, Rahman N. The NSD1 and EZH2 overgrowth genes, similarities and differences. *Am J Med Genet C* 2013; **163C**: 86–91.
13 Zamorano-León JJ, Yañez R, Jaime G, Rodriguez-Sierra P, Calatrava-Ledrado L, Alvarez-Granada RR *et al.* KCNH2 gene mutation: a potential link between epilepsy and long QT-2 syndrome. *J Neurogenet* 2012; **26**: 382–386.
14 Burwinkel B, Scott JW, Bührer C, van Landeghem FK, Cox GF, Wilson CJ *et al.* Fatal congenital heart glycogenosis caused by a recurrent activating R531Q mutation in the gamma 2-subunit of AMP-activated protein kinase (PRKAG2), not by phosphorylase kinase deficiency. *Am J Hum Genet* 2005; **76**: 1034–1049.
15 Li F, Shen Y, Köhler U, Sharkey FH, Menon D, Coulleaux L *et al.* Interstitial microduplication of Xp22.31: causative of intellectual disability or benign copy number variant? *Eur J Med Genet* 2010; **53**: 93–99.
16 Dubourg C, Lazaro L, Pasquier L, Bendavid C, Blayau M, Le Duff F *et al.* Molecular screening of SHH, ZIC2, SIX3, and TGIF genes in patients with features of holoprosencephaly spectrum: Mutation review and genotype-phenotype correlations. *Hum Mutat* 2004; **24**: 43–51.
17 Metherell LA, Chan LF, Clark AJ. The genetics of ACTH resistance syndromes. *Best Pract Res Clin Endocrinol Metab* 2006; **20**: 547–560.
18 Yeste D, González-Niño C, Pérez de Nanclares G, Pérez-Nanclares G, Audi L, Castaño L *et al.* ACTH-dependent precocious pseudopuberty in an infant with DAX1 gene mutation. *Eur J Pediatr* 2009; **168**: 65–69.

19 O'Shaughnessy PJ, Fleming LM, Jackson G, Hochgeschwender U, Reed P, Baker PJ. Adrenocorticotropic hormone directly stimulates testosterone production by the fetal and neonatal mouse testis. *Endocrinology* 2003; **144**: 3279–3284.
20 Silveira LF, Trarbach EB, Latronico AC. Genetics basis for GnRH-dependent pubertal disorders in humans. *Mol Cell Endocrinol* 2010; **324**: 30–38.

Supplemental Information for this article can be found on the *Human Genome Variation* website (http://www.nature.com/hgv).

Molecular Genetics & Genomic Medicine

Open Access

ORIGINAL ARTICLE

Testicular dysgenesis/regression without campomelic dysplasia in patients carrying missense mutations and upstream deletion of *SOX9*

Yuko Katoh-Fukui[1,a], Maki Igarashi[1,a], Keisuke Nagasaki[2], Reiko Horikawa[3], Toshiro Nagai[4], Takayoshi Tsuchiya[4], Erina Suzuki[1], Mami Miyado[1], Kenichiro Hata[5], Kazuhiko Nakabayashi[5], Keiko Hayashi[5], Yoichi Matsubara[6], Takashi Baba[7], Ken-ichirou Morohashi[7], Arisa Igarashi[8], Tsutomu Ogata[1,9], Shuji Takada[8] & Maki Fukami[1]

[1]Department of Molecular Endocrinology, National Research Institute for Child Health and Development, Tokyo, Japan
[2]Division of Pediatrics, Department of Homeostatic Regulation and Development, Niigata University Graduate School of Medical and Dental Sciences, Niigata, Japan
[3]Division of Endocrinology and Metabolism, National Center for Child Health and Development, Tokyo, Japan
[4]Department of Pediatrics, Dokkyo Medical University Koshigaya Hospital, Koshigaya, Japan
[5]Department of Maternal-Fetal Biology, National Research Institute for Child Health and Development, Tokyo, Japan
[6]National Research Institute for Child Health and Development, Tokyo, Japan
[7]Department of Molecular Biology, Graduate School of Medical Sciences, Kyushu University, Fukuoka, Japan
[8]Department of Systems BioMedicine, National Research Institute for Child Health and Development, Tokyo, Japan
[9]Department of Pediatrics, Hamamatsu University School of Medicine, Hamamatsu, Japan

Keywords
Campomelic dysplasia, deletion, enhancer, mutation, testis

Correspondence
Maki Fukami, Department of Molecular Endocrinology, National Research Institute for Child Health and Development, Tokyo, Japan. Tel: +81-3-5494-7025;
Fax: +81-3-5494-7026;
E-mail: fukami-m@ncchd.go.jp

Funding Information
This study was funded by the Grant-in-Aid from the Ministry of Education, Culture, Sports, Science and Technology; by the Grant-in-Aid from the Japan Society for the Promotion of Science; by the Grants from the Ministry of Health, Labour and Welfare, from the National Center for Child Health and Development and from the Takeda Foundation.

Received: 23 April 2015; Revised: 15 June 2015; Accepted: 16 June 2015

***Molecular Genetics & Genomic Medicine* 2015; 3(6): 550–557**

doi: 10.1002/mgg3.165

[a]These authors contributed equally to this study.

Abstract

SOX9 haploinsufficiency underlies campomelic dysplasia (CD) with or without testicular dysgenesis. Current understanding of the phenotypic variability and mutation spectrum of *SOX9* abnormalities remains fragmentary. Here, we report three patients with hitherto unreported *SOX9* abnormalities. These patients were identified through molecular analysis of 33 patients with 46,XY disorders of sex development (DSD). Patients 1–3 manifested testicular dysgenesis or regression without CD. Patients 1 and 2 carried probable damaging mutations p.Arg394Gly and p.Arg437Cys, respectively, in the *SOX9* C-terminal domain but not in other known 46,XY DSD causative genes. These substitutions were absent from ~120,000 alleles in the exome database. These mutations retained normal transactivating activity for the *Col2a1* enhancer, but showed impaired activity for the *Amh* promoter. Patient 3 harbored a maternally inherited ~491 kb *SOX9* upstream deletion that encompassed the known 32.5 kb XY sex reversal region. Breakpoints of the deletion resided within nonrepeat sequences and were accompanied by a short-nucleotide insertion. The results imply that testicular dysgenesis and regression without skeletal dysplasia may be rare manifestations of *SOX9* abnormalities. Furthermore, our data broaden pathogenic *SOX9* abnormalities to include C-terminal missense substitutions which lead to target-gene-specific protein dysfunction, and enhancer-containing upstream microdeletions mediated by nonhomologous end-joining.

Introduction

SOX9 (OMIM *608160) controls embryonic development by transactivating several genes such as *COL2A1* involved in skeletal formation and *AMH* involved in testicular development. Known *SOX9* mutations include various missense substitutions in the high-mobility group or dimerization domains, as well as several nonsense, frameshift, and splice-site mutations widely distributed in the coding region (Meyer et al. 1997; Bernard et al. 2003; Harley et al. 2003; Michel-Calemard et al. 2004; Staffler et al. 2010). Patients with *SOX9* mutations manifest campomelia, hypoplastic scapulae, pelvic anomalies, micrognathia, and cleft palate, collectively referred to as campomelic dysplasia (CD), although a certain percentage of mutation-positive patients show a mild variant of CD that lacks campomelia (acampomelic CD: ACD) (Bernard et al. 2003; Michel-Calemard et al. 2004; Staffler et al. 2010). *SOX9* mutations also result in complete or partial gonadal dysgenesis in individuals with 46,XY karyotype (Meyer et al. 1997; Michel-Calemard et al. 2004). As CD/ACD-compatible skeletal abnormalities were described in all patients with *SOX9* mutations and disorders of sex development (DSD) were shared only by ~70% of 46,XY patients (Mansour et al. 1995), it seems that skeletal tissues are more vulnerable than testis to impaired SOX9 function. Kwok et al. (1996) suggested that *SOX9* mutations are unlikely to underlie 46,XY DSD in the absence of skeletal abnormalities.

Recent studies have identified submicroscopic deletions in the *SOX9* upstream region in six patients with isolated 46,XY DSD (Pop et al. 2004; Lecointre et al. 2009; Kim et al. 2015). These patients shared a 32.5 kb overlapping region of deletion at a position 607–640 kb upstream of the *SOX9* start codon, which was designated as the XY sex reversal region (XYSR). Since *SOX9* expression is regulated by multiple tissue-specific enhancers (Bagheri-Fam et al. 2006), XYSR likely contains a testis-specific enhancer. Considering the limited number of reported patients, further studies are necessary to clarify the phenotypic variability and mutation spectrum of *SOX9* abnormalities. Furthermore, the genomic basis of *SOX9* upstream deletions remains to be investigated. Here, we report three unique cases with *SOX9* abnormalities.

Materials and Methods

Subjects

This study was approved by the Institutional Review Board Committee at the National Center for Child Health and Development. The study group consisted of 33 Japanese patients with 46,XY DSD. All patients showed genital abnormalities at birth; of these, 29 had isolated DSD, whereas the remaining patients manifested DSD with additional clinical features. Eleven and 22 patients were raised as a female and male, respectively. Patients with apparent chromosomal abnormalities were excluded from this study.

Mutation analysis

After obtaining written informed consent from the patients or their parents, genomic DNA samples were collected from the patients. Mutation analysis was performed by next-generation sequencing (NGS). Genomic DNA samples were isolated from peripheral leukocytes. Target regions in the human genome were amplified with the SureSelect Target Enrichment system (G7531C or all exome v5; Agilent Technologies, Palo Alto, CA) and sequenced on a HiSeq 2000 sequencer (Illumina, San Diego, CA). Nucleotide alterations were called by Avadis NGS 1.3.1 (DNA Chip Research, Yokohama, Japan) or SAMtools 0.1.17 software (http://samtools.sourcefrge.net/). In this study, we focused on protein-altering substitutions and splice-site mutations of 27 known causative genes for 46,XY DSD, that is, *AKR1C2*, *AKR1C4*, *AMH*, *AMHR2*, *AR*, *ATF3*, *ATRX*, *BNC2*, *CYP11A1*, *DHH*, *DMRT1*, *GATA4*, *HSD3B2*, *HSD17B3*, *INSL3*, *INSR*, *LHCGR*, *MAP3K1*, *NR5A1*, *POR*, *RXFP2*, *SOX9*, *SRD5A2*, *SRY*, *STAR*, *TSPYL1*, and *WT1*. Nucleotide substitutions of allele frequency 1% or higher in the Japanese population (Human Genetic Variation Browser, http://www.genome.med.kyoto-u.ac.jp/SnpDB) were excluded as polymorphisms. *SOX9* (NM_000346.3) mutations indicated by NGS were confirmed by Sanger sequencing using a primer pair: SOX9-exon3FW2 (5′-CAGGCGCACACGCTGACCAC-3′) and SOX9-exon3RV (5′-CCTCTCTTTCTTCGGTTAT-3′). Furthermore, PCR products carrying the nucleotide alterations were subcloned into the TOPO TA cloning vector (Life Technologies, Carlsbad, CA) and the mutant and wild-type alleles were sequenced separately. Whenever possible, parental samples of mutation-positive patients were also subjected to molecular analysis.

Functional analyses of *SOX9* substitutions

Conservation and functional consequences of *SOX9* substitutions were predicted using Polyphen-2 (http://genetics.bwh.harvard.edu/pph2/) (Adzhubei et al. 2010). Population frequencies of the substitutions were analyzed using the Exome Aggregation Consortium Browser (http://exac.broadinstitute.org/).

The transactivating activity of the substitutions was assessed by a previously reported method with modifications (Kelberman et al. 2006). Briefly, an expression vector for wild-type *SOX9* was purchased from Origene Technologies (RC208944, Rockville, MD), and each *SOX9* mutation was introduced into the expression vector by site-directed mutagenesis (PrimeSTAR Mutagenesis Basal Kit; Takara Bio, Ohtsu, Japan). In this study, we compared the transactivating activity of newly identified mutants to that of the known ACD-associated *SOX9* mutant c.527C>T (p.Pro176Leu) (Michel-Calemard et al. 2004). We used a PGL3 reporter vector (Promega, Madison, WI) containing the murine *Amh* promoter sequence (from −231 to 0 to the transcription start site of *Amh*, NC_000076.6) and a PGL4 reporter vector (Promega) containing the murine *Col2a1* enhancer sequence (from +1958 to +2485 to the transcription start site of *Col2a1*, NC_000081.6). An expression vector for *NR5A1* was kindly provided by Professor Toshihiko Yanase (Fukuoka University, Fukuoka, Japan). Luciferase assays for the *Amh* promoter and for the *Col2a1* enhancer were carried out using COS-1 (RIKEN, Ibaraki, Japan) and HEK293 cells (Health Science Research Resources Bank, Tokyo, Japan), respectively. The cells were seeded in 6-well dishes and treated with Lipofectamine 2000 Reagent (Life Technologies). For *Amh* promoter assays, we transfected cells with 40 ng *SOX9* expression vector, 100 ng *NR5A1* expression vector, 1 μg reporter vector, and 3 ng pCMV-PRL control vector (Promega). For *Col2a1* enhancer assays, we used 200 ng *SOX9* expression vector, 500 ng reporter vector, and 3 ng pCMV-PRL vector. At 48 h after transfection, luciferase activity was measured using the Dual-Luciferase Reporter Assay System (Promega) with Lumat LB9507 (Berthold, Oak Ridge, TN). Every assay was performed in triplicate and all experiments were repeated at least three times. The results are expressed as the mean ± one standard deviation, and statistical significance was calculated by the Student *t* test. *P* values of <0.005 were considered significant.

Copy-number analysis

Copy-number alterations were analyzed by comparative genomic hybridization using a catalog human array (4 × 180 k format) or a custom-made array (design ID, 031687) (Agilent Technologies). The deletion breakpoints were determined by direct sequencing of PCR products harboring the fusion junction. The products were generated using a primer pair: 5′-TTTTTTCCTTGAAGTTAATG-3′ and 5′-AATGTAGTGCTATATATTGC-3′. Sizes and genomic positions of the deletions were analyzed using the UCSC genome browser (http://genome.ucsc.edu/; GRCh37/hg19) and the presence or absence of repeat sequences was examined with RepeatMasker (http://www.repeatmasker.org). We referred to the Database of Genomic Variants (http://projects.tcag.ca/variation/) to exclude known benign variants.

Results

Mutation analysis

We identified two heterozygous missense substitutions c.1180C>G (p.Arg394Gly) and c.1309C>T (p.Arg437Cys) in patients 1 and 2, respectively, in *SOX9* (Fig. 1). These substitutions have not been reported previously. Patients 1 and 2 carried no mutations in the other genes examined or in other nucleotides of *SOX9*. The substitution of patient 2 was shared by the phenotypically normal mother, whereas parental samples of patient 1 were not available for genetic analysis. The p.Arg394Gly and p.Arg437Cys substitutions resided within the proline/glutamine/serine (PQS)-rich domain (also known as SPQ-rich domain) at the C-terminus (McDowall et al. 1999) (Fig. 1A).

Functional analysis of *SOX9* substitutions

The c.1180C>G (p.Arg394Gly) and c.1309C>T (p.Arg437Cys) substitutions involved highly conserved amino acids, and were predicted as "probably damaging" by in silico analyses (Fig. 1B). These substitutions were absent from ~120,000 alleles of the exome database. The p.Arg394Gly and p.Arg437Cys mutants retained normal in vitro transactivating activity for the *Col2a1* enhancer (relative fold activation: 1.14 and 1.17, respectively), but exerted impaired activity for the *Amh* promoter (relative fold activation: 0.74 and 0.81, respectively) (Fig. 1C). In contrast, the previously reported ACD-associated p.Pro176Leu mutant showed markedly reduced activity for both reporters (relative fold activation: 0.50 for the *Col2al* enhancer and 0.26 for the *Amh* promoter).

Copy-number analysis

We identified a heterozygous deletion in the upstream region of *SOX9* in patient 3 (Fig. 1D). The deletion was 490,990 bp in physical length and started at a position 380,011 bp upstream to the *SOX9* start codon (chr17: 69,246,534–69,737,523; GRCh37/hg19). The deletion encompassed the known XYSR (Figs. 1D, 2). The deletion breakpoints resided in nonrepeat sequences and shared no homology (Fig. 1D). The fusion junction was accompanied by a short-nucleotide insertion of unknown origin that was indicative of an "information scar" of nonhomologous end-joining (NHEJ) (Lieber 2008). Patient 3

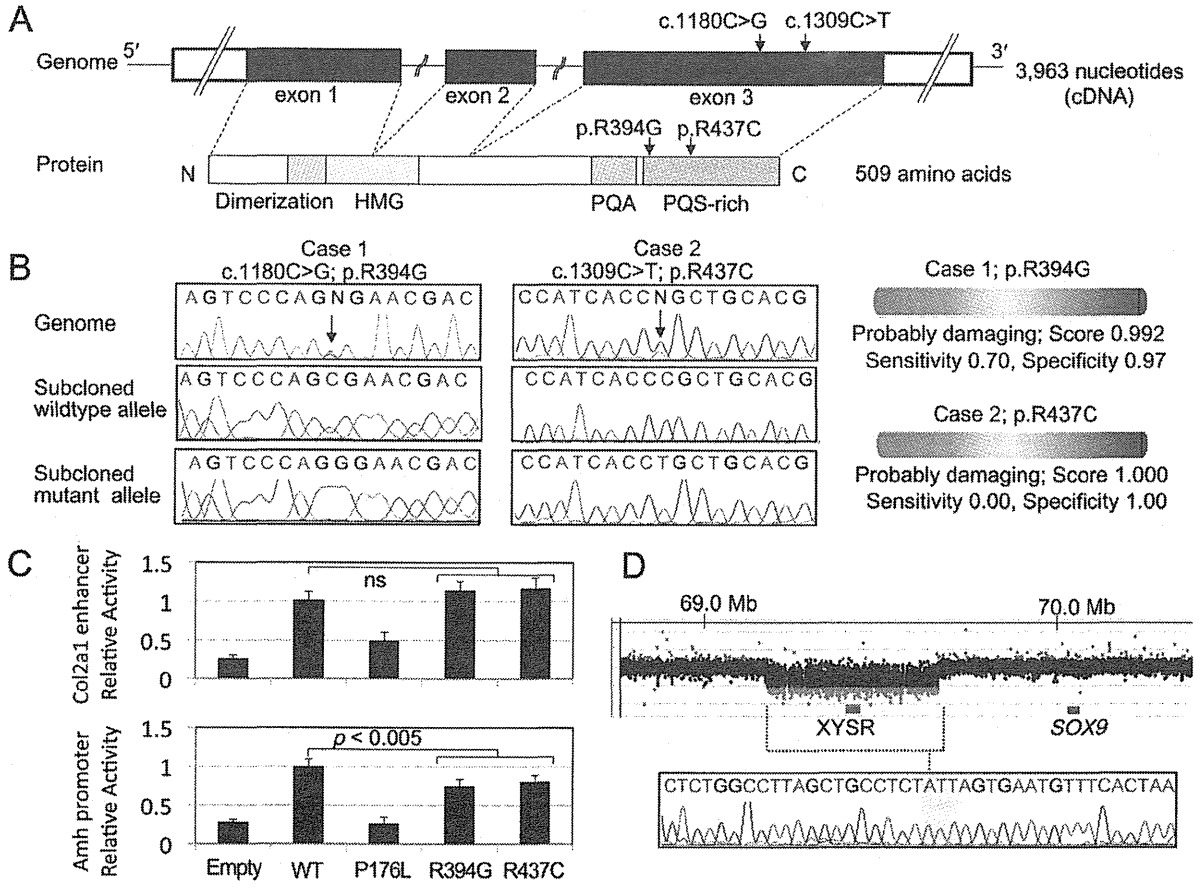

Figure 1. *SOX9* abnormalities in patients 1–3. (A) Genomic and protein structures of *SOX9*/SOX9. The positions of the c.1180C>G (p.Arg394Gly) and c.1309C>T (p.Arg437Cys) mutations are indicated by arrows. White and black boxes in the upper panel indicate the untranslated and coding regions, respectively. Colored boxes in the lower panel indicate dimerization (codon 60–101) (Bernard et al. 2003), high-mobility group (HMG: codon 101–184), proline/glutamine/alanine (PQA: codon 339–379), and proline/glutamine/serine-rich (PQS-rich: codon 386–509) domains (McDowall et al. 1999). (B) Nucleotide substitutions detected in patients 1 and 2. Left panel: electro chromatograms of the mutations. The mutated nucleotides are indicated by arrows. Right panel: in silico functional prediction of mutant proteins. (C) In vitro assays using reporters containing the *Col2a1* enhancer or *Amh* promoter. The transactivating activity of p.Arg394Gly and p.Arg437Cys mutants was compared to that of the known ACD-associated SOX9 mutant p.Pro176Leu (Michel-Calemard et al. 2004). The results are expressed as the mean ± one standard deviation. Relative transactivating activities of the SOX9 mutants against the wild-type are shown. Empty: empty expression vector; ns: not significant. (D) *SOX9* upstream deletion in patient 3. Upper panel: array-based comparative genomic hybridization analysis. The black, red, and green dots denote signals indicative of the normal, increased (> +0.5) and decreased (< −1.0) copy-numbers, respectively. The blue and red boxes represent previously reported XY sex reversal region (XYSR) (Kim et al. 2015) and *SOX9* exons, respectively. Genomic positions refer to the UCSC database (http://genome.ucsc.edu/; GRCh37/hg19). Lower panel: sequence of the fusion junction. The junction is accompanied by a short-nucleotide insertion of unknown origin (the red-shaded area).

carried no sequence alteration in all genes examined. The *SOX9* upstream deletion was identified in the phenotypically normal mother of patient 3.

Clinical features of the mutation-positive patients

Physical and hormonal findings of patients 1–3 are summarized in Table 1. Blood inhibin B levels were not determined in these cases. Patient 1 was a 19-year-old individual raised as a male. He manifested hypospadias and bilateral cryptorchidism at birth and underwent surgical intervention at 5 years of age. At 14 years of age, he was subjected to endocrine evaluation because of a lack of pubertal sexual development. Blood examinations revealed increased levels of gonadotropins and mildly decreased levels of testosterone, indicating testicular dysfunction. He began to receive testosterone supplementation therapy at

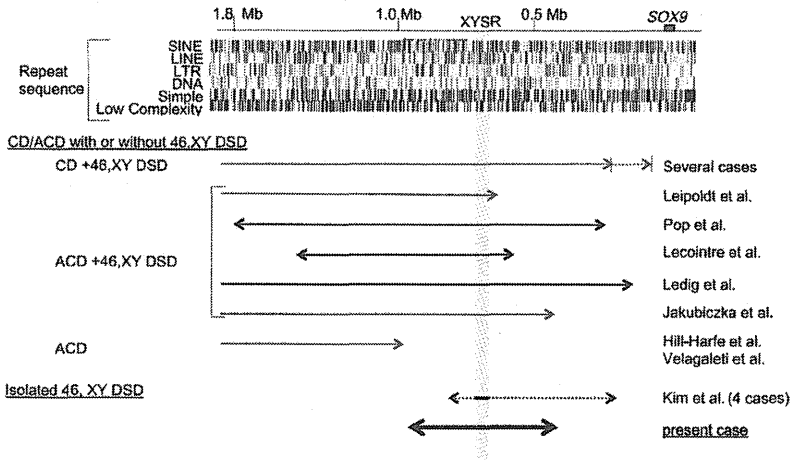

Figure 2. Schematic representation of the *SOX9* upstream region. Upper panel represents positions of *SOX9* and repeat sequences (UCSC database, http://genome.ucsc.edu/; GRCh37/hg19). The numbers indicate the distance from *SOX9*. Lower panel represents genomic rearrangements in the present and previous cases. Blue and black arrows indicate chromosomal translocations and deletions, respectively. Broken arrows indicate breakpoint regions of multiple patients. The red-shaded area represents the XYSR reported by Kim et al. (2015). XYSR, XY sex reversal region; CD, campomelic dysplasia; ACD, acampomelic CD; DSD, disorders of sex development.

age 14, and human chorionic gonadotropin and human menopausal gonadotropin therapy at age 16. He underwent surgical intervention for gynecomastia at 14 and 16 years of age. Abdominal ultrasound at 18 years of age showed small testes with focal microlithiasis. Müllerian duct derivatives were absent. He had no skeletal abnormalities except for spina bifida occulta, a relatively common neural tube anomaly of that has not been associated with *SOX9* mutations (Greene and Copp 2014).

Patient 2 was a 5-year-old male individual. At birth, he showed male-type external genitalia; however, bilateral testes were not palpable in the scrotum or in the inguinal region. At 2.6 years of age, laparoscopic examination detected possible gonadal remnants with spermatic cord in the bilateral inguinal canals. Histological examination of biopsied samples showed that the possible remnants were fibrous tissues without germ cells. At 2.8 years of age, he was referred to our clinic for further evaluation. He showed normal skeletal features and borderline micropenis. Endocrine analyses revealed increased gonadotropin levels and undetectable levels of testosterone and anti-Müllerian hormone. Abdominal imaging did not detect a uterus or gonads. Thus, this patient was diagnosed with testicular regression. At 5 years of age, he was capable of voiding in a standing position.

Patient 3 was a 22-year-old individual with a female phenotype. Her growth and development were uneventful until pubertal age. At 13 years of age, she visited our clinic because of a lack of pubertal sexual development. She showed normal skeletal features and female-type external genitalia. Endocrine evaluation indicated severe gonadal dysfunction. Abdominal magnetic resonance imaging detected a uterus of a prepubertal size. Estrogen supplementation therapy from 14 years of age successfully induced breast budding and vaginal bleeding. Gonadectomy was performed at 17 years of age. Histological examination revealed bilateral dysgenic gonads with seminoma.

Discussion

This study provides several notable findings. This is the first report documenting the association between *SOX9* intragenic mutations and isolated 46,XY DSD. In vitro assays confirmed the target-specific functional impairment of the c.1180C>G (p.Arg394Gly) and c.1309C>T (p.Arg437Cys) mutants, which were not observed in the known ACD-associated mutant c.527C>T (p.Pro176Leu). Notably, unlike other known pathogenic *SOX9* missense mutations, p.Arg394Gly and p.Arg437Cys resided within the C-terminal PQS-rich domain. As the PQS-rich domain is required for SOX9 interaction with other proteins (Tsuda et al. 2003), the two mutations may affect SOX9-mediated protein–protein interactions in the developing testis. Physical and hormonal findings of patients 1 and 2 with these mutations were indicative of impaired testicular development, although blood inhibin B levels, a sensitive marker for the function of the testis (Grinspon et al. 2012), were not determined in these patients.

It is worth mentioning that patient 2 manifested bilateral testicular regression, a rare form of 46,XY DSD that probably occurs as a result of the disturbance of developmental processes during testicular tubule formation (Mizuno et al. 2012). The genetic basis of testicular regression remains unknown, with the exception of *NR5A1* muta-

Table 1. Molecular and clinical findings of patients 1–3.

	Patient 1		Patient 2		Patient 3	
Karyotype	46,XY		46,XY		46,XY	
Molecular defects in *SOX9* (NM_000346.3)	c.1180C>G (p.Arg394Gly)		c.1309C>T (p.Arg437Cys)		Upstream deletion	
Physical findings at birth						
External genitalia	Male-type genitalia with hypospadias and unpalpable testes		Male-type genitalia with micropenis and unpalpable testes		Complete female-type genitalia	
Physical findings at later ages						
Age at exam. (year)	19		2.8		22	
Penile size (cm)[1]	**5.7**[2] (8.6–10.0)		**2.5** (3.0–3.6)		Not examined	
Testicular size (mL)	5 (right), 3–4 (left)[3]		Not palpable		Not palpable	
Gonadal histology	Not analyzed		Fibrous tissues		Streak gonad with seminoma	
Uterus	Absent		Absent		Present	
Additional findings	Spina bifida occulta		None		None	
Hormonal findings[1]						
Age at exam. (year)	19		2.8		13	
	B	S	B	S	B	S
LH (mIU/mL)[4]	*37.5* (0.5–5.0)	*126.6* (6.0–21.0)	*2.8* (<0.3–1.3)	Not analyzed	*13.8* (<0.2–2.1)	*119.4* (1.3–7.0)
FSH (mIU/mL)[4]	*17.7* (0.8–4.4)	*24.3* (1.5–8.0)	*109.8* (0.4–1.5)	Not analyzed	*82.5* (<0.3–3.0)	*135.8* (1.3–3.9)
Testosterone (ng/mL)[5]	5.3 (2.5–11.0)	**4.9** (6.3–9.8)	**<0.03** (0.06–0.16)	**<0.03** (>0.2)	**0.09** (0.68–1.22)	**0.16** (2.96–5.58)
AMH (ng/mL)	Not analyzed	Not analyzed	**<0.1** (74.1–148.1)	<0.1 (no data)	Not analyzed	Not analyzed

The conversion factor to the SI unit: LH 1.0 (IU/L), FSH 1.0 (IU/L), testosterone 3.47 (nmol/L), and AMH 7.14 (pmol/L). Penile size and hormone values below the reference range are boldfaced, and hormone values above the reference range are italicized. B, basal; S, stimulated; LH, luteinizing hormone; FSH, follicle-stimulating hormone; AMH, anti-Müllerian hormone.

[1]Reference ranges are shown in parentheses.

[2]After hormone replacement therapy.

[3]After surgical interventions.

[4]Gonadotropin releasing hormone stimulation test (100 $\mu g/m^2$, max. 100 μg bolus i.v.; blood sampling at 0, 30, 60, 90, and 120 min).

[5]Human chorionic gonadotropin stimulation test (3000 IU/m^2, max. 5000 IU i.m. for three consecutive days; blood sampling on days 1 and 4).

tions that account for a minor fraction of cases (Philibert et al. 2007). It has been suggested that testicular regression and gonadal dysgenesis are a continuum of a disorder (Marcantonio et al. 1994). Indeed, *NR5A1* mutations are known to underlie both conditions (Ferraz-de-Souza et al. 2011). Animal studies suggested that SOX9 plays a role in testicular tubule differentiation through the interaction with SOX8 (Barrionuevo et al. 2009). Moreover, SOX9 plays a critical role not only in testicular development but also in the maintenance of differentiated status of the testes (Sekido and Lovell-Badge 2009; Veitia 2010). Thus, testicular regression may be a rare manifestation in patients with *SOX9* mutations. However, this notion is based on the findings of a single individual, and therefore awaits further investigation.

One may argue against p.Arg394Gly and p.Arg437Cys being responsible for the severe DSD in patients 1 and 2 because these mutations resulted in only modest decrease in the transactivating activity for the *AMH* promoter. The discrepancy between the phenotypic severities and the results of in vitro assays can be explained by assuming that some SOX9 target genes other than *AMH* are more sensitive to defective function of SOX9. Actually, a number of testicular genes are known to be regulated by SOX9 (Sekido and Lovell-Badge 2009; Veitia 2010). Alternatively, in the developing testis, the p.Arg394Gly and p.Arg437Cys mutations may disrupt the synergic interaction between SOX9 and certain cofactors. It is known that SOX9 synergizes with other proteins to transactivate target genes (Sekido and Lovell-Badge 2009; Veitia 2010). On the other hand, we cannot exclude the possibility that genetic variations in other genes or some environmental factors affected sexual development in patients 1 and 2, although mutations in known 46,XY DSD causative genes were excluded in these patients. Further studies, including in vitro assays using reporter vectors containing various SOX9 target promoters and expression vectors for several SOX9 cofactors, and whole exome sequencing of patients 1 and 2, will clarify the precise functional consequences of the mutants.

The findings in patient 3 support the notion that the 32.5 kb XYSR contains a DNA element(s) essential for testicular development. Moreover, exclusion mapping indicates that *SOX9* enhancers for skeletal tissues and craniofacial regions are located outside of the ~491 kb region deleted in patient 3 (Fig. 2) (Pop et al. 2004; Hill-Harfe et al. 2005; Velagaleti et al. 2005; Lecointre et al. 2009; Jakubiczka et al. 2010; Ledig et al. 2010; Kim et al. 2015). In addition, the results of this study, together with those of previous studies (Pop et al. 2004; Lecointre et al. 2009; Kim et al. 2015) provide evidence of the genomic heterogeneity of *SOX9* upstream deletions. The breakpoint sequences in patient 3 suggest that the deletion resulted from NHEJ. Actually, genomic regions around *SOX9* are not enriched with repeat sequences that serve as substances of nonallelic homologous recombination (Fig. 2). Thus, NHEJ may be the major cause of *SOX9* upstream microdeletions, although other mechanisms such as microhomology-mediated replication errors may also be involved in the development of such deletions. Since all known pathogenic deletions in the *SOX9* upstream region, including that in our patient, were transmitted from phenotypically normal mothers of the patients (Kim et al. 2015), de novo occurrence of such deletions seems to be a rare event.

In summary, the results indicate that the phenotypic consequences of *SOX9* mutations are broader than previously reported and include testicular dysgenesis and regression without skeletal dysplasia. Furthermore, our data suggest that DSD-associated *SOX9* abnormalities include C-terminal missense substitutions that lead to target-specific protein dysfunction, and NHEJ-mediated upstream microdeletions encompassing XYSR.

Acknowledgments

This study was funded by the Grant-in-Aid from the Ministry of Education, Culture, Sports, Science and Technology; by the Grant-in-Aid from the Japan Society for the Promotion of Science; by the Grants from the Ministry of Health, Labour and Welfare, from the National Center for Child Health and Development and from the Takeda Foundation.

Conflict of Interest

None declared.

References

Adzhubei, I. A., S. Schmidt, L. Peshkin, V. E. Ramensky, A. Gerasimova, P. Bork, et al. 2010. A method and server for predicting damaging missense mutations. Nat. Methods 7:248–249.

Bagheri-Fam, S., F. Barrionuevo, U. Dohrmann, T. Gunther, R. Schule, R. Kemler, et al. 2006. Long-range upstream and downstream enhancers control distinct subsets of the complex spatiotemporal Sox9 expression pattern. Dev. Biol. 291:382–397.

Barrionuevo, F., I. Georg, H. Scherthan, C. Lecureuil, F. Guillou, M. Wegner, et al. 2009. Testis cord differentiation after the sex determination stage is independent of Sox9 but fails in the combined absence of Sox9 and Sox8. Dev. Biol. 327:301–312.

Bernard, P., P. Tang, S. Liu, P. Dewing, V. R. Harley, and E. Vilain. 2003. Dimerization of SOX9 is required for chondrogenesis, but not for sex determination. Hum. Mol. Genet. 12:1755–1765.

Ferraz-de-Souza, B., L. Lin, and J. C. Achermann. 2011. Steroidogenic factor-1 (SF-1, NR5A1) and human disease. Mol. Cell. Endocrinol. 336:198–205.

Greene, N. D., and A. J. Copp. 2014. Neural tube defects. Annu. Rev. Neurosci. 37:221–242.

Grinspon, R. P., N. Loreti, D. Braslavsky, P. Bedecarrás, V. Ambao, S. Gottlieb, et al. 2012. Sertoli cell markers in the diagnosis of paediatric male hypogonadism. J. Pediatr. Endocrinol. Metab. 25:3–11.

Harley, V. R., M. J. Clarkson, and A. Argentaro. 2003. The molecular action and regulation of the testis-determining factors, SRY (sex-determining region on the Y chromosome) and SOX9 [SRY-related high-mobility group (HMG) box 9]. Endocr. Rev. 24:466–487.

Hill-Harfe, K. L., L. Kaplan, H. J. Stalker, R. T. Zori, R. Pop, G. Scherer, et al. 2005. Fine mapping of chromosome 17 translocation breakpoints > or = 900 Kb upstream of SOX9 in acampomelic campomelic dysplasia and a mild, familial skeletal dysplasia. Am. J. Hum. Genet. 76:663–671.

Jakubiczka, S., C. Schroder, R. Ullmann, M. Volleth, S. Ledig, E. Gilberg, et al. 2010. Translocation and deletion around SOX9 in a patient with acampomelic campomelic dysplasia and sex reversal. Sex Dev. 4:143–149.

Kelberman, D., K. Rizzoti, A. Avilion, M. Bitner-Glindzicz, S. Cianfarani, J. Collins, et al. 2006. Mutations within Sox2/SOX2 are associated with abnormalities in the hypothalamo-pituitary-gonadal axis in mice and humans. J. Clin. Invest. 116:2442–2455.

Kim, G. J., E. Sock, A. Buchberger, W. Just, F. Denzer, W. Hoepffner, et al. 2015. Copy number variation of two separate regulatory regions upstream of SOX9 causes isolated 46, XY or 46, XX disorder of sex development. J. Med. Genet. 52:240–247.

Kwok, C., P. N. Goodfellow, and J. R. Hawkins. 1996. Evidence to exclude SOX9 as a candidate gene for XY sex reversal without skeletal malformation. J. Med. Genet. 33:800–801.

Lecointre, C., O. Pichon, A. Hamel, Y. Heloury, L. Michel-Calemard, Y. Morel, et al. 2009. Familial acampomelic form of campomelic dysplasia caused by a 960 kb deletion upstream of SOX9. Am. J. Med. Genet. A 149A:1183–1189.

Ledig, S., O. Hiort, G. Scherer, M. Hoffmann, G. Wolff, S. Morlot, et al. 2010. Array-CGH analysis in patients with syndromic and non-syndromic XY gonadal dysgenesis: evaluation of array CGH as diagnostic tool and search for new candidate loci. Hum. Reprod. 25:2637–2646.

Lieber, M. R. 2008. The mechanism of human nonhomologous DNA end joining. J. Biol. Chem. 283:1–5.

Mansour, S., C. M. Hall, M. E. Pembrey, and I. D. Young. 1995. A clinical and genetic study of campomelic dysplasia. J. Med. Genet. 32:415–420.

Marcantonio, S. M., P. Y. Fechner, C. J. Migeon, E. J. Perlman, and G. D. Berkovitz. 1994. Embryonic testicular regression sequence: a part of the clinical spectrum of 46, XY gonadal dysgenesis. Am. J. Med. Genet. 49:1–5.

McDowall, S., A. Argentaro, S. Ranganathan, P. Weller, S. Mertin, S. Mansour, et al. 1999. Functional and structural studies of wild type SOX9 and mutations causing campomelic dysplasia. J. Biol. Chem. 274:24023–24030.

Meyer, J., P. Sudbeck, M. Held, T. Wagner, M. L. Schmitz, F. D. Bricarelli, et al. 1997. Mutational analysis of the SOX9 gene in campomelic dysplasia and autosomal sex reversal: lack of genotype/phenotype correlations. Hum. Mol. Genet. 6:91–98.

Michel-Calemard, L., G. Lesca, Y. Morel, D. Boggio, H. Plauchu, and J. Attia-Sobol. 2004. Campomelic acampomelic dysplasia presenting with increased nuchal translucency in the first trimester. Prenat. Diagn. 24:519–523.

Mizuno, K., Y. Kojima, H. Kamisawa, S. Kurokawa, Y. Moritoki, H. Nishio, et al. 2012. Feasible etiology of vanishing testis regarding disturbance of testicular development: histopathological and immunohistochemical evaluation of testicular nubbins. Int. J. Urol. 19:450–456.

Philibert, P., D. Zenaty, L. Lin, S. Soskin, F. Audran, J. Leger, et al. 2007. Mutational analysis of steroidogenic factor 1 (NR5a1) in 24 boys with bilateral anorchia: a French collaborative study. Hum. Reprod. 22: 3255–3261.

Pop, R., C. Conz, K. S. Lindenberg, S. Blesson, B. Schmalenberger, S. Briault, et al. 2004. Screening of the 1 Mb SOX9 5′ control region by array CGH identifies a large deletion in a case of campomelic dysplasia with XY sex reversal. J. Med. Genet. 41:e47.

Sekido, R., and R. Lovell-Badge. 2009. Sex determination and SRY: down to a wink and a nudge? Trends Genet. 25:19–29.

Staffler, A., M. Hammel, M. Wahlbuhl, C. Bidlingmaier, A. W. Flemmer, P. Pagel, et al. 2010. Heterozygous SOX9 mutations allowing for residual DNA-binding and transcriptional activation lead to the acampomelic variant of campomelic dysplasia. Hum. Mutat. 31: E1436–E1444.

Tsuda, M., S. Takahashi, Y. Takahashi, and H. Asahara. 2003. Transcriptional co-activators CREB-binding protein and p300 regulate chondrocyte-specific gene expression via association with Sox9. J. Biol. Chem. 278: 27224–27229.

Veitia, R. A. 2010. FOXL2 versus SOX9: a lifelong "battle of the sexes". Bioessays 32:375–380.

Velagaleti, G. V., G. A. Bien-Willner, J. K. Northup, L. H. Lockhart, J. C. Hawkins, S. M. Jalal, et al. 2005. Position effects due to chromosome breakpoints that map approximately 900 Kb upstream and approximately 1.3 Mb downstream of SOX9 in two patients with campomelic dysplasia. Am. J. Hum. Genet. 76:652–662.

SCIENTIFIC REPORTS

OPEN

Parturition failure in mice lacking *Mamld1*

Mami Miyado[1], Kenji Miyado[2], Momori Katsumi[1], Kazuki Saito[1], Akihiro Nakamura[2], Daizou Shihara[1], Tsutomu Ogata[1,3] & Maki Fukami[1]

Received: 05 June 2015
Accepted: 07 September 2015
Published: 05 October 2015

In mice, the onset of parturition is triggered by a rapid decline in circulating progesterone. Progesterone withdrawal occurs as a result of functional luteolysis, which is characterized by an increase in the enzymatic activity of 20α-hydroxysteroid dehydrogenase (20α-HSD) in the corpus luteum and is mediated by the prostaglandin F2α ($PGF_{2\alpha}$) signaling. Here, we report that the genetic knockout (KO) of *Mamld1*, which encodes a putative non-DNA-binding regulator of testicular steroidogenesis, caused defective functional luteolysis and subsequent parturition failure and neonatal deaths. Progesterone receptor inhibition induced the onset of parturition in pregnant KO mice, and MAMLD1 regulated the expression of *Akr1c18*, the gene encoding 20α-HSD, in cultured cells. Ovaries of KO mice at late gestation were morphologically unremarkable; however, *Akr1c18* expression was reduced and expression of its suppressor *Stat5b* was markedly increased. Several other genes including *Prlr*, *Cyp19a1*, *Oxtr*, and *Lgals3* were also dysregulated in the KO ovaries, whereas $PGF_{2\alpha}$ signaling genes remained unaffected. These results highlight the role of MAMLD1 in labour initiation. MAMLD1 likely participates in functional luteolysis by regulating *Stat5b* and other genes, independent of the $PGF_{2\alpha}$ signaling pathway.

In most mammals including mice, uterine quiescence during pregnancy is maintained by circulating progesterone synthesized primarily in the ovarian luteal cells[1,2]. Progesterone binds to its receptor in the uterus and suppresses the expression of genes involved in myometrial contraction[3,4]. Previous studies have shown that signal transducer and activator of transcription 5b (STAT5B) is essential to sustain blood progesterone levels in pregnant mice[5–7]. STAT5B inhibits ovarian expression of *Akr1c18*, the gene for 20α-hydroxysteroid dehydrogenase (20α-HSD) that converts progesterone into an inactive metabolite 20α-hydroxyprogesterone (20α-OHP)[5]. From 18 days post coitum (dpc), *i.e.*, 24–36 hours before term, progesterone secretion from the ovary progressively declines through processes referred to as functional and structural luteolysis[1,5]. Functional luteolysis is an enzymatic shift characterized by an increase in 20α-HSD activity[1,5]. This process is followed by structural luteolysis, in which the corpus luteum undergoes morphological changes and cellular apoptosis[1,8]. To date, multiple molecules have been implicated in functional luteolysis[1]. Of these, prostaglandin F2α ($PGF_{2\alpha}$) upregulates *Akr1c18* via a signaling pathway consisting of $PGF_{2\alpha}$, $PGF_{2\alpha}$ receptor (FP), JUND, and nuclear receptor subfamily 4 group A member 1 (NR4A1, also known as NUR77)[1,9,10]. The Gq/11 protein family also serves as a component of the $PGF_{2\alpha}$ signaling pathway[11]. Genetic knockout (KO) of *Akr1c18*, *Fp*, or $G\alpha_{q/11}$ leads to persistent progesterone production and subsequent parturition failure[5,11–13]. In addition, *Fp* KO perturbs expression of several steroidogenic genes in the corpus luteum, which may also be relevant to delayed parturition[14]. Other factors, including NOTCH 1 and 4, oxytocin receptor (OXTR), and galectin 3, also participate in luteolytic processes and/or regulation of *Akr1c18*[1,15–17]; however, it remains unknown whether STAT5B plays a role in functional luteolysis.

[1]Department of Molecular Endocrinology, National Research Institute of Child Health and Development, Tokyo 157-8535, Japan. [2]Department of Reproductive Biology, National Research Institute of Child Health and Development, Tokyo 157-8535, Japan. [3]Department of Pediatrics, Hamamatsu University School of Medicine, Hamamatsu 431-3192, Japan. Correspondence and requests for materials should be addressed to M.F. (email: fukami-m@ncchd.go.jp)

Genotype of mother	Genotype of father	Delayed parturition[a]	Statistical significance[b]
WT	WT	4/21[c]	
Mamld1 KO	WT	6/11	$p = 0.040$
Mamld1 KO	*Mamld1* KO	14/24	$p = 0.027$
WT	*Mamld1* KO	2/11[c]	$p = 0.83$

Table 1. Frequency of delayed parturition. WT: wildtype; KO: knockout. [a]The denominators indicate the number of pregnant mice, and the numerators are the number of mice with delayed parturition (≥20.5 days post coitum). [b]The results are compared to that of WT pairs. [c]The frequency of delayed parturition in WT animals was comparable between this study and previous studies[3,24].

MAMLD1 on the human X chromosome (NM_001177465) is a causative gene for disorders of sex development in 46,XY individuals[18]. Loss-of-function mutations in *MAMLD1* have been identified in male patients with hypospadias[18–20]. Murine *Mamld1* (NM_001081354) also resides on the X chromosome and is strongly expressed in the Leydig and Sertoli cells of the fetal testis[18]. *In vitro* knockdown assays using mouse Leydig tumour cells (MLTC1) and *in vivo* analysis of male *Mamld1* KO mice indicated that MAMLD1 transactivates several Leydig cell-specific genes including *Star*, *Cyp11a1*, *Cyp17a1*, *Hsd3b1*, and *Insl3* without exerting a demonstrable DNA-binding capacity[21–23]. While male *Mamld1* KO mice showed no hypospadias, the phenotypic difference between human patients and KO mice was explicable by species differences in the process of male sex development[23]. To date, the function of MAMLD1 in females has not been investigated, although previous analyses detected strong expression of *Mamld1* in the ovaries of adult mice[18]. In the present study, we analyzed phenotypic and molecular characteristics of female *Mamld1* KO mice.

Results

***Mamld1* KO causes parturition failure in female mice.** Prior to this study, we generated a mouse strain in which the genomic structure of *Mamld1* was disrupted by substituting a *PGK-neo* cassette for *Mamld1* exon 3 that corresponds to approximately two-thirds of the coding region[23]. We have reported that male *Mamld1* KO mice retained normal external genitalia and fertility, despite having mildly impaired expression of Leydig cell-specific genes in the fetal testis[23].

In this study, we analyzed the phenotype of female *Mamld1* KO mice. The mice were healthy and exhibited no discernible anomalies. Furthermore, the mice were fertile when mated with male wildtype (WT) or *Mamld1* KO mice. However, female KO mice frequently showed delayed parturition (Table 1). More than 50% of KO mice gave birth to their first pups at 20.5 dpc or later, while approximately 80% of WT animals gave birth at 19.5 dpc. The frequency of delayed parturition (≥20.5 dpc) in WT animals was comparable between this study and previous studies[3,24]. The genotype of the mated male mice (WT or KO) had no influence on the parturition timing of the female WT or KO mice.

Pups born to *Mamld1* KO mothers have a high neonatal mortality rate and can be rescued by caesarean operation. We examined the number of pups born to WT and *Mamld1* KO mothers. Although the average number of pups at birth was comparable between the two groups, the average number of pups alive at postnatal day 1 was significantly lower in KO mothers (Fig. 1a,b). Approximately half of the pups born to *Mamld1* KO mothers died within the first 24 hours after birth, while >80% of pups born to WT mothers survived beyond this period. The dead pups of KO mothers exhibited no apparent malformations (Fig. 1a). Most pups survived beyond postnatal day 1 remained alive until adulthood. The newborn mortality rates of WT and KO mothers were not affected by paternal genotype (WT or KO). The sex ratio of the dead pups was almost 1:1. Thus, the neonatal deaths were more likely the result of an aberrant maternal condition rather than inborn defects in the pups.

It is known that parturition failure in female *Ptgfr* KO mice results in frequent fetal death[12,13]. To clarify whether the high mortality rate of pups born to *Mamld1* KO mothers was due to delayed parturition, we performed caesarean operations on the day of the expected term (19.5 dpc). The operations significantly improved the survival rate of pups; at postnatal day 1, the average number of live pups born to the operated KO mothers was comparable to that born to non-operated WT mothers (Fig. 1b).

Progesterone withdrawal is impaired in pregnant *Mamld1* KO mice. Previous studies have shown that parturition failure is caused by defects in functional luteolysis that lead to persistent progesterone production[5,12,13,15,24]; however, it can also be caused by uterine lesions such as defective myometrial contraction or delayed cervical ripening[25,26]. To determine whether progesterone withdrawal is impaired in pregnant *Mamld1* KO mice, we measured serum levels of progesterone and other steroids. In this study, we utilized liquid chromatography tandem mass spectrometry (LC-MS/MS), which is more sensitive and accurate than conventional immunoassays[27]. Serum samples were collected from pregnant WT and KO mice at 18.5 dpc, a stage at which circulating progesterone usually declines in WT mice[25].

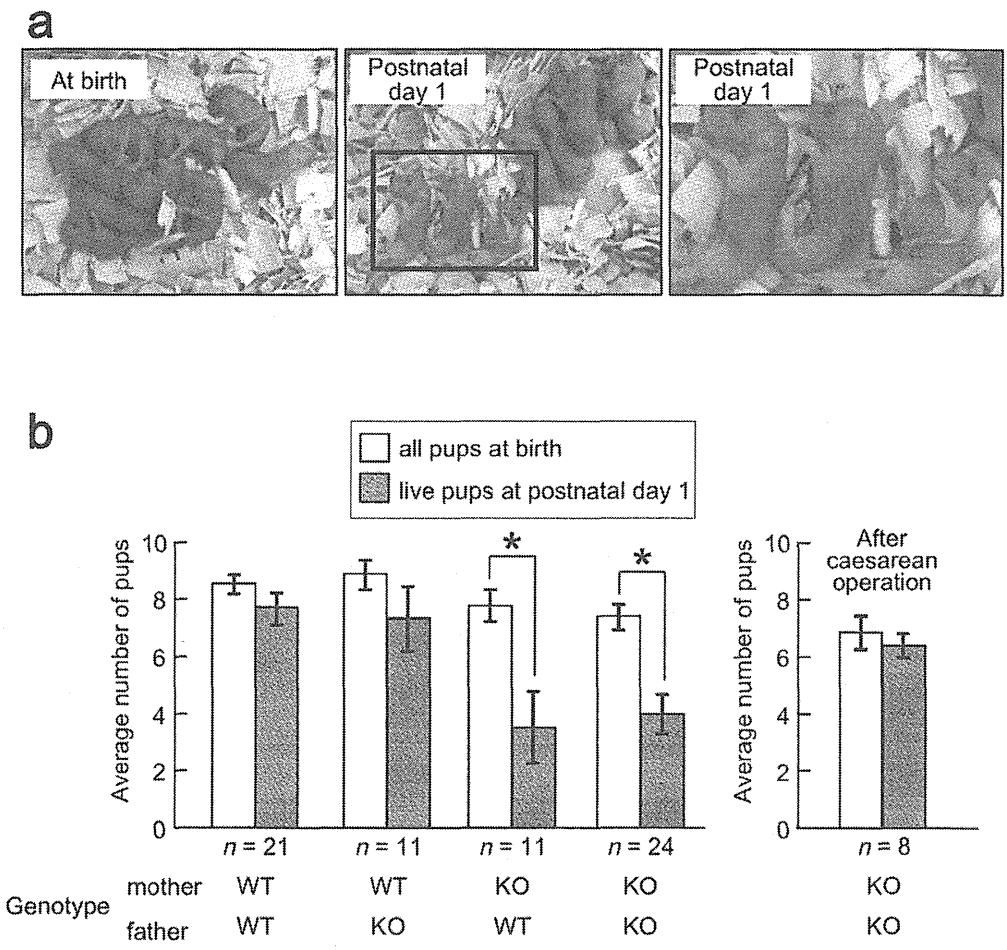

Figure 1. Phenotypes of pups born to *Mamld1* knockout (KO) mothers. (**a**) Pups born to KO mothers at 20.5 dpc. Pups showed a high neonatal mortality, although they had no congenital anomalies. The photographs were taken by M.M. and M.F. at the National Research Institute for Child Health and Development. (**b**) Average number of births (white bars) and that of live pups at postnatal day 1 (gray bars). Pups born to KO mothers showed a significantly higher newborn mortality rate than those born to wildtype (WT) mothers (asterisks). Paternal genotype had no effect on the number of pups. Frequent newborn deaths were eliminated by caesarean operation. The results are expressed as the mean ± SEM.

Serum progesterone was significantly higher in KO mice than in WT animals (Table 2). In contrast, serum levels of 20α-OHP, the inactive metabolite of progesterone, remained low in KO mice. Altered serum levels of progesterone and 20α-OHP were also observed in KO mice at 20.5 dpc (Table 2). Blood levels of testosterone and estradiol were comparable between WT and KO mice.

To confirm that impaired progesterone withdrawal is the major cause of parturition failure in *Mamld1* KO mice, we treated pregnant mice with the progesterone receptor antagonist RU486. Administration of 150 μg RU486 at 17.5 or 18.5 dpc invariably induced vaginal bleeding (the signs of labour initiation) and/or delivery of a pup(s) within 24 hours in both WT and KO mice (Supplementary Table S1).

We also examined whether *Mamld1* KO affects ovarian structures. The size and appearance of the ovaries were comparable between pregnant WT and KO mice at 18.5 dpc (Fig. 2a,b). No apparent histological changes were observed in the ovaries of KO mice (Fig. 2c–f). Furthermore, the average number of corpora lutea in the ovary and that of implants in the uterus were similar between WT and KO mice (Fig. 2g). The position of uterine implantation was also normal in KO mice. These data indicate that *Mamld1* KO exerts a deleterious effect on functional luteolysis, but not on ovary development, ovulation, luteinization or implantation.

In ovaries of WT mice during late gestation, *Mamld1* is continuously expressed, while expression levels of *Akr1c18*, *Nr4a1*, and *Stat5b* drastically change after 17.5 dpc. We examined *Mamld1* expression in the ovaries of WT mice at late gestation. Real-time PCR detected continuous expression in the ovaries, with the highest expression at 17.5 dpc (Fig. 3a). *In situ* hybridization of the

	Genotype		Statistical significance
18.5 days post coitum[a]			
	WT ($n=10$)	*Mamld1* KO ($n=9$)	
Progesterone (ng/mL)	10.9 ± 3.6	26.8 ± 2.6	$p=0.0014$
20α-OHP (ng/mL)	37.0 ± 5.5	20.6 ± 2.1	$p=0.041$
Testosterone (pg/mL)	214.7 ± 25.8	272.5 ± 43.3	$p=0.87$
Estradiol (pg/mL)	27.6 ± 3.8	24.8 ± 4.4	$p=0.63$
20.5 days post coitum[b]			
	WT ($n=4$)	*Mamld1* KO ($n=5$)	
Progesterone (ng/mL)	4.9 ± 2.6	23.0 ± 8.8	$p=0.050$
20α-OHP (ng/mL)	39.4 ± 4.3	26.2 ± 5.8	$p=0.13$

Table 2. Serum steroid hormone levels in WT and *Mamld1* KO mice. WT: wildtype; KO: knockout; 20α-OHP: 20α-hydroxyprogesterone. The results are expressed as the mean ± SEM. [a]During pregnancy. [b]WT mice, at 0 or 1 day postpartum; KO mice, during pregnancy.

murine ovary at 18.5 dpc showed clear signals for *Mamld1* mRNA in the corpora lutea as well as in the primary, secondary, vesicular, and mature follicles (Fig. 3b–d).

We also analyzed mRNA levels of *Akr1c18*, *Nr4a1*, and *Stat5b* in ovaries of pregnant WT mice at 17.5 and 18.5 dpc. These genes showed drastic changes in expression between 17.5 and 18.5 dpc, as reported previously[10]. *Akr1c18* and *Nr4a1* expression was significantly higher at 18.5 dpc than at 17.5 dpc, while *Stat5b* expression was markedly decreased at 18.5 dpc (Fig. 3f).

In addition, we analyzed *Mamld1* expression in the uteri of pregnant WT mice at 18.5 dpc. A relatively weak expression was detected in the uteri, as compared to that in the ovaries (Fig. 3g).

MAMLD1 regulates *Akr1c18* expression *in vivo* and *in vitro*. We examined the expression of *Akr1c18*/20α-HSD in pregnant WT and *Mamld1* KO mice at 18.5 dpc. Real-time PCR analysis showed significantly decreased *Akr1c18* expression in the whole ovaries and corpora lutea of KO mice (Fig. 4a), and Western blot analysis confirmed the reduction of 20α-HSD protein expression in the ovaries of KO mice (Supplementary Fig. S1). In contrast, mRNA levels of *Akr1c18* in the uteri were comparable between WT and KO mice at 18.5 dpc (Fig. 4b). Expression of *Srd5a1* for steroid 5α reductase, which mediates local progesterone metabolism in the uterus, remained unaffected in KO mice (Fig. 4b). *Akr1c18* expression remained low in the KO mice at 20.5 dpc (Supplementary Fig. S2).

To confirm the effect of MAMLD1 on *Akr1c18* expression, we performed *in vitro* assays. In these experiments, we used MLTC1, which has high endogenous expression of both *Mamld1* and *Akr1c18*. First, we carried out knockdown assays using two siRNAs for *Mamld1*. When *Mamld1* mRNA levels were suppressed to ~25% by the siRNAs, *Akr1c18* mRNA levels were reduced to ~75% (Fig. 4c). Next, we performed *Mamld1* overexpression experiments. Transient transfection with a *Mamld1* expression vector resulted in a ~2-fold increase of *Akr1c18* mRNA after a 24-hour cell culture (Fig. 4d).

***Mamld1* KO dysregulates *Stat5b* and other genes in the ovaries of pregnant mice.** We examined gene expression patterns in the whole ovaries and corpora lutea of pregnant WT and *Mamld1* KO mice at 18.5 dpc (Fig. 5). The most remarkable changes in KO mice were the significantly increased mRNA levels of *Stat5b*, despite overexpression of *Socs3*, which encodes a putative inhibitor of *Stat5*. *Prlr* and *Esr1* were also upregulated. In contrast, *Fp*, *Jund*, and *Nr4a1* were not affected, except for a slightly decreased expression of *Jund* in the whole ovaries. Increased levels of STAT5B protein and unaffected levels of NR4A1 protein in KO mice ovaries were confirmed by Western blot analysis (Supplementary Fig. S1). Markedly increased *Stat5b* mRNA expression was also observed in pregnant KO mice at 20.5 dpc (Supplementary Fig. S2).

We also analyzed mRNA levels of other genes involved in ovarian steroidogenesis and in the luteolytic processes (Figs 5 and 6). Gene expression patterns were grossly similar in the whole ovaries and corpora lutea. Among the steroidogenic genes, *Cyp19a1* was significantly upregulated. Expression levels of *Hsd17b3*, *Hsd17b1*, and *Hsd17b7* were mildly increased, while mRNA levels of *Cyp11a1* and *Cyp17a1* remained unchanged. *Star* expression was slightly decreased, but only in the whole ovaries. Of the genes involved in the luteolytic processes, *Oxtr* was upregulated, while *Lgals3* encoding anti-apoptotic factor galectin 3 was downregulated. *Notch 1* and *4* were unaffected.

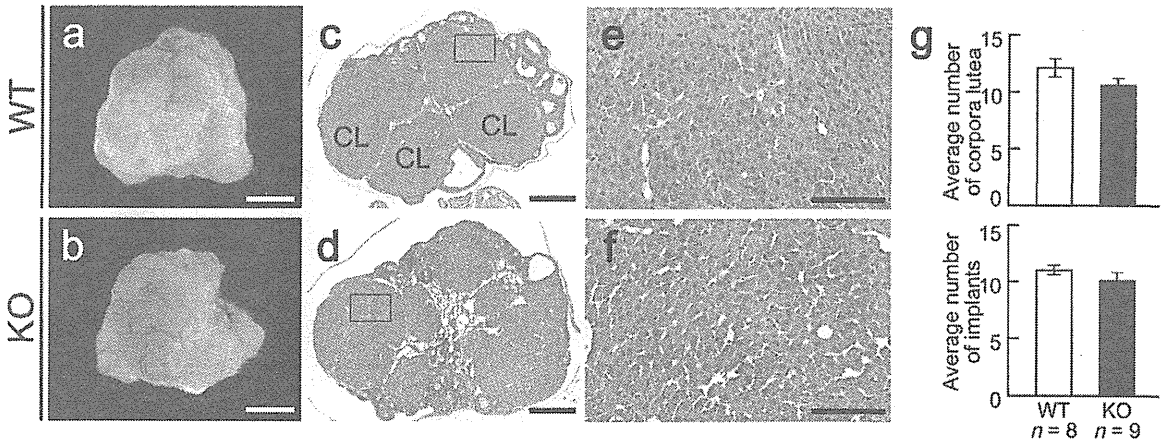

Figure 2. Morphological analysis. (**a–f**) Morphological findings of the ovaries obtained from pregnant WT and *Mamld1* KO mice at 18.5 dpc. Scale bars: 1 mm (**a,b**), 500 μm (**c,d**), and 100 μm (**e,f**). CL, corpus luteum. (**g**) Average number of corpora lutea in the ovary (upper panel) and that of implants in the uterus (lower panel) at 18.5 dpc. The results are expressed as the mean ± SEM.

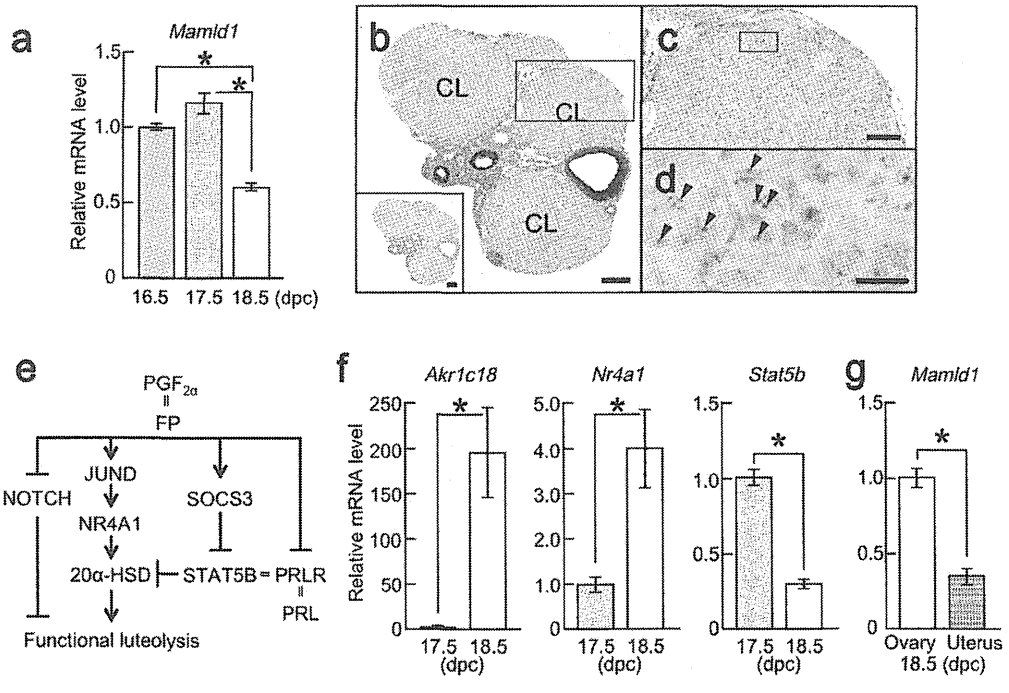

Figure 3. *Mamld1* expression in pregnant WT mice. (**a**) *Mamld1* expression in whole ovaries from pregnant WT mice at 16.5 ($n = 3$), 17.5 ($n = 5$), and 18.5 dpc ($n = 8$). mRNA levels relative to that of *Gapdh* are shown. The results are expressed as the mean ± SEM. The average of mRNA levels at 16.5 dpc was defined as 1.0. Asterisks indicate statistical significance. (**b–d**) *Mamld1* expression in corpora lutea and follicles. Arrowheads indicate *Mamld1* signals in corpus luteum. Scale bars: 200 μm (**b**), 100 μm (**c**), and 20 μm (**d**). No specific expression of the negative control (a sense probe). CL, corpus luteum. (**e**) Known factors involved in functional luteolysis. Arrow and bar headed lines indicate stimulatory and inhibitory effects, respectively. Double lines indicate protein-receptor bindings. FP, prostaglandin F2α receptor; PRL, prolactin; PRLR, PRL receptor. (**f**) Gene expression in the whole ovaries in pregnant WT mice at 17.5 and 18.5 dpc ($n = 5$ and 8, respectively). The average of mRNA levels at 17.5 dpc was defined as 1.0. (**g**) *Mamld1* expression in the whole ovaries (Ovary, $n = 8$) and uteri (Uterus, $n = 4$) from pregnant WT mice at 18.5 dpc. The average of mRNA levels in the whole ovaries was defined as 1.0.

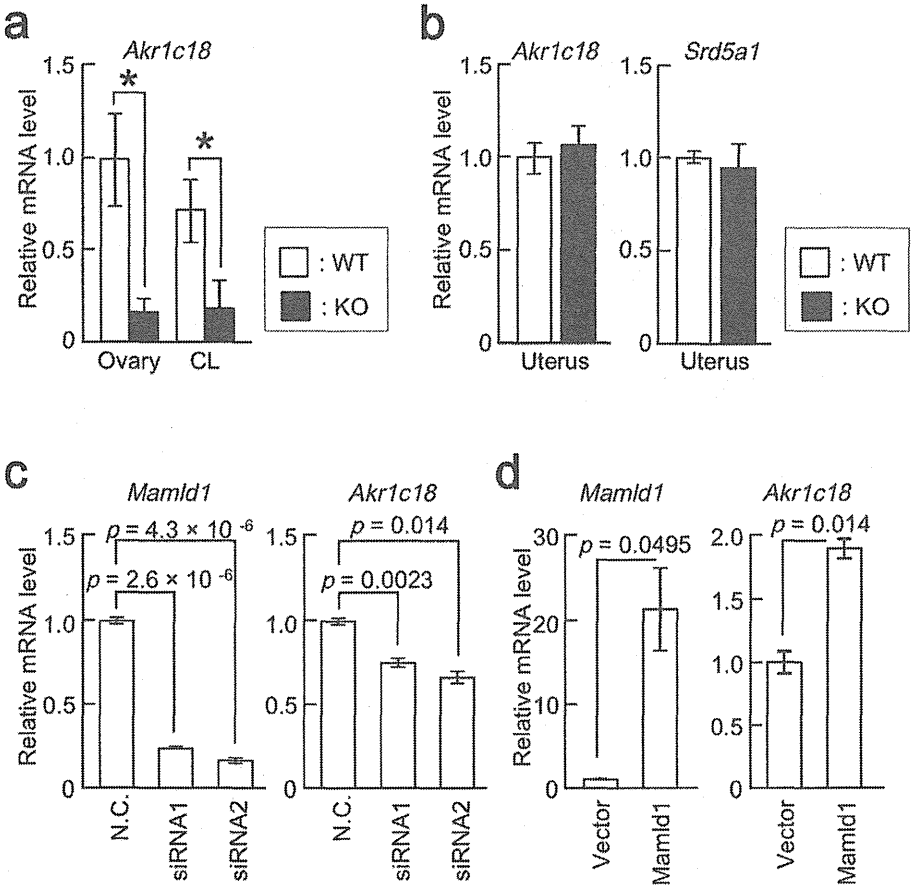

Figure 4. The effect of MAMLD1 on *Akr1c18* expression. (**a**) *Akr1c18* expression in the whole ovaries (Ovary) and corpora lutea (CL) of pregnant WT ($n = 8$, white bars) and *Mamld1* KO ($n = 9$, black bars) mice at 18.5 dpc. mRNA levels relative to that of *Gapdh* are shown. The results are expressed as the mean ± SEM. The average of mRNA levels in the whole ovaries of WT mice was defined as 1.0. Significant differences between WT and KO animals are indicated by asterisks. (**b**) *Akr1c18* and *Srd5a1* expression in the uteri (Uterus) of pregnant WT ($n = 4$, white bars) and KO ($n = 4$, black bars) mice at 18.5 dpc. The average of mRNA levels in WT mice was defined as 1.0. (**c**) *Mamld1* knockdown assays. N.C., negative control (non-targeting siRNA). The average of mRNA levels in N.C. was defined as 1.0. (**d**) Overexpression experiments of *Mamld1*. Vector, empty expression vector. The average of mRNA levels in Vector was defined as 1.0.

Discussion

Targeted deletion of *Mamld1* in female mice caused parturition failure and frequent neonatal deaths without affecting ovarian morphology. This phenotype likely results from attenuated functional luteolysis, because expression of *Akr1c18* mRNA and 20α-HSD protein was markedly decreased in the ovaries of pregnant *Mamld1* KO mice at 18.5 dpc. Consistent with this, ratios of 20α-OHP to progesterone in blood samples were lower in KO mice than in WT animals. Although the serum levels of progesterone and 20α-OHP in our mice differed from those in previous reports[5,10], this can be ascribed to the difference in the methods (LC-MS/MS vs. conventional immunoassays) and sampling points (the day when a vaginal plug was observed was designated as 0.5 dpc in this study and as 1.0 dpc in previous studies). Attenuated functional luteolysis seemed to persist in KO mice after the day of the expected term. We found that inhibition of progesterone signaling by RU486 induced vaginal bleeding (the signs of labour initiation) and/or delivery of a pup(s) in KO mice. *In vitro* assays indicated that MAMLD1 upregulates *Akr1c18* in MLTC1, although these results need to be confirmed in further studies using cells of ovarian origin. While previous studies have shown that local progesterone metabolism in the uterus can also affect parturition timing[25,26], mRNA levels of *Akr1c18* and *Srd5a1* in the uteri remained unaffected in *Mamld1* KO mice. Furthermore, *Mamld1* was continuously expressed in the ovaries during late gestation, and only weakly expressed in the uteri. Collectively, the results suggest that MAMLD1 is involved in upregulation of *Akr1c18* in ovaries of pregnant mice at late gestation.

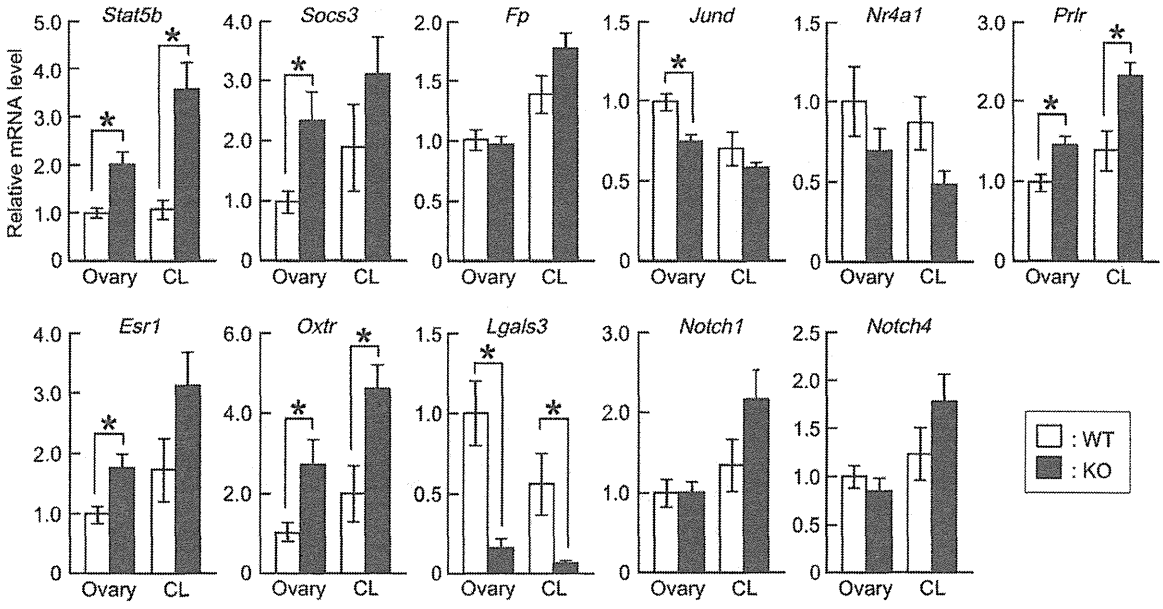

Figure 5. Expression patterns of functional luteolysis-related genes in pregnant WT and *Mamld1* KO mice. Relative mRNA levels of genes in the whole ovaries (Ovary) and corpora lutea (CL) in pregnant WT ($n = 6$, white bars) and KO ($n = 6$, black bars) mice at 18.5 dpc are shown. The results are expressed as the mean ± SEM. The average of mRNA levels in the whole ovaries of WT mice was defined as 1.0. Asterisks indicate statistical significance.

The phenotype of pregnant *Mamld1* KO mice overlaps with that of *Fp* KO mice[12,13]; however, expression of the $PGF_{2\alpha}$ signaling pathway genes, *Fp*, *Jund*, and *Nr4a1*, was not significantly altered in the ovaries of *Mamld1* KO mice at 18.5 dpc. Likewise, protein expression of NR4A1, the most downstream component of the $PGF_{2\alpha}$ signaling pathway that directly binds to the *Akr1c18* promoter, remained unaffected in KO mice ovaries. Thus, the function of MAMLD1 appears to be independent of the $PGF_{2\alpha}$ signaling pathway, although mRNA expression of the Gq/11 protein family, a recently identified component of this pathway[11], was not analyzed in the present study. In contrast, *Stat5b* and *Prlr* were markedly upregulated in KO mice ovaries. Increased *Prlr* expression can be ascribed to high STAT5B activity, which transactivates *Prlr*[28]. Likewise, *Esr1*, the potential target of STAT5B in rats[29], was also upregulated in *Mamld1* KO mice. To date, STAT5B has not been implicated in functional luteolysis, although it suppresses *Akr1c18* during mid-gestation[5]. We confirmed that *Stat5b* expression significantly declined in pregnant WT mice ovaries after 17.5 dpc. Our data imply that *Stat5b* suppression mediated by MAMLD1 is critical for functional luteolysis. Since MAMLD1 protein transactivates various genes in the fetal testis without demonstrable DNA binding capacity[21,23], MAMLD1 may regulate *Stat5b* expression as a non-DNA-binding co-activator. In this regard, it is noteworthy that the phenotypic severity of pregnant *Mamld1* KO mice was milder than that of *Fp* KO mice. While *Mamld1* KO permits a term delivery in approximately half of pregnant mice, *Fp* KO leads to parturition failure and loss of pups in all mice[12,13]. Likewise, the increase in blood progesterone levels at the end of pregnancy was less significant in *Mamld1* KO mice than in *Fp* KO mice. These results are consistent with the findings that *Akr1c18* mRNA levels in the ovaries were decreased by 70–80% in pregnant *Mamld1* KO mice, and by 100% in *Fp* KO mice[10]. This suggests that although MAMLD1 and $PGF_{2\alpha}$ signaling are essential for the luteolytic process, the role of MAMLD1 is relatively minor compared to that of $PGF_{2\alpha}$ signaling.

Several other genes were dysregulated in pregnant *Mamld1* KO mice ovaries. First, *Cyp19a1*, *Hsd17b3*, *Hsd17b1*, and *Hsd17b7* involved in ovarian steroidogenesis were upregulated. These molecular alterations did not affect blood sex hormone levels. However, perturbed steroidogenesis may play a role in parturition failure of *Mamld1* KO mice, because previous studies suggested that the androgen:estrogen synthesis ratio in the ovaries affects the luteolytic process[14]. Second, *Oxtr* expression was increased in the KO mice ovaries. It has been shown that administration of low-dose oxytocin results in persistent progesterone production and subsequent parturition failure, whereas high-dose oxytocin causes uterine contraction and early labour[12]. Since downregulation of *Oxtr* in the ovaries and its upregulation in the uteri were proposed to induce the onset of parturition[2,30], elevated expression of *Oxtr* in the ovaries of *Mamld1* KO mice may be associated with delayed parturition. Third, expression of *Lgals3* was decreased in the whole ovaries and corpora lutea of KO mice. *Lgals3* is co-expressed with *Akr1c18* in the corpora lutea, and galectin 3 encoded by *Lgals3* contributes to the elimination of luteal cells[8]. Thus, decreased

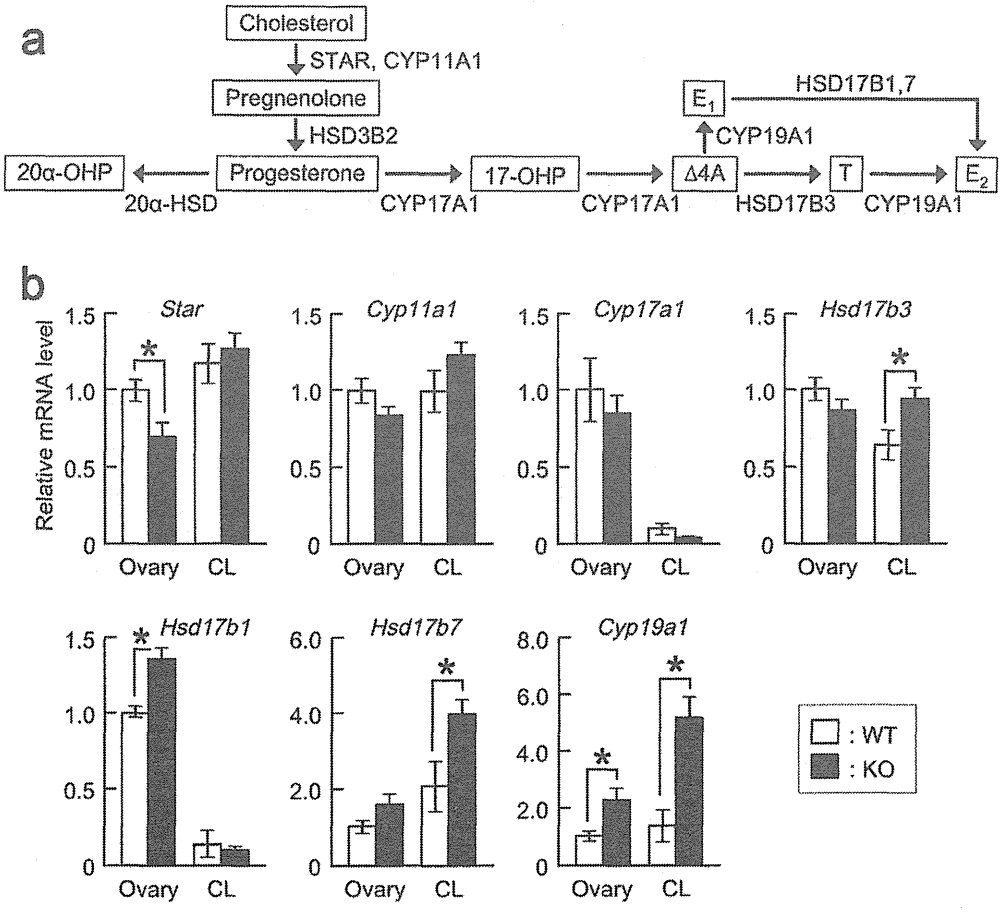

Figure 6. Expression patterns of steroidogenic genes in pregnant WT and *Mamld1* KO mice. (**a**) Enzymes involved in the steroidogenic pathway. 17-OHP, 17-hydroxyprogesterone; 20α-OHP, 20α-hydroxyprogesterone; E_1, estrone; Δ4A, androstenedione; T, testosterone; E_2, estradiol. (**b**) Gene expression in the whole ovaries (Ovary) and corpora lutea (CL) in pregnant WT ($n = 6$, white bars) and KO ($n = 6$, black bars) mice at 18.5 dpc. mRNA levels relative to that of *Gapdh* are shown. The results are expressed as the mean ± SEM. The average of mRNA levels in the whole ovaries of WT mice was defined as 1.0. Significant differences between WT and KO animals are indicated by asterisks. *Hsd3b2* was undetectable in both WT and KO mice.

Lgals3 expression in the ovaries of *Mamld1* KO mice may also be relevant to impaired luteolysis. Lastly, expression of *Notch 1* and *4* remained intact in KO mice. Thus, although MAMLD1 has sequence similarity with a Notch co-factor Mastermind-like 2[21], the function of MAMLD1 in the ovaries is unlikely to be associated with Notch signals.

In summary, our results indicate that MAMLD1-mediated *Stat5b* suppression is essential for term delivery in mice. MAMLD1 appears to participate in a complex molecular network in the ovaries and regulate functional luteolysis, without affecting expression of $PGF_{2\alpha}$ signaling genes. This study provides novel insights into molecular mechanisms of mammalian reproduction.

Methods

Treatment of animals. Animal experiments in this study were approved by the Animal Care Committee at the National Research Institute for Child Health and Development (project number: A2008-001). All experiments were performed in accordance with the institutional guidelines of the care and use of laboratory animals. All mice were housed under specific pathogen-free controlled conditions with a 12-hour light-dark cycle. Food and water were available *ad libitum*.

***Mamld1* KO mice.** Male *Mamld1* KO mice were generated by targeting deletion of exon 3[23]. The mice were backcrossed with the C57BL/6N strain (Sankyo Labo Service Corp. Inc., Tokyo, Japan).

Cross-mating and caesarean operation. Cross-mating was performed between female *Mamld1* KO mice and male WT or KO mice and between female WT mice and male WT or KO mice. Female mice from 7 to 25 weeks of age and male mice from 8 to 40 weeks of age were used for mating. The noon of the day when a vaginal plug was observed was designated as 0.5 dpc. Vaginal bleeding (the signs of labour initiation) or delivery of the first pup was defined as the onset of parturition. Caesarean operation was performed for *Mamld1* KO mice at 19.5 dpc. After birth, the pups were nursed by lactating WT animals.

Measurement of serum steroid metabolites. Blood samples were collected from the right ventricle of the heart of euthanized pregnant WT and KO mice at 18.5 dpc, pregnant KO mice at 20.5 dpc, and WT mice at 0 or 1 day postpartum. The serum was separated by centrifugation and stored at −80 °C until hormone measurements were performed. Serum steroid metabolites were measured by LC-MS/MS (ASKA Pharma Medical, Kanagawa, Japan).

Parturition induction by progesterone receptor antagonist. The progesterone receptor antagonist RU486 (mifepristone; Sigma-Aldrich, St. Louis, MO) was administered to pregnant mice at 17.5 or 18.5 dpc. One ml of solution containing 150 μg RU486 in 6% ethanol was subcutaneously injected in the bilateral hind legs.

Morphological and quantitative analyses of corpora lutea and uterine implants. We analyzed the morphology of ovaries obtained from pregnant WT and KO mice at 18.5 dpc. Tissue samples were fixed with 4% paraformaldehyde, dehydrated, and embedded in paraffin. Serial 6 μm sections were mounted on microscope slides. The samples were stained with hematoxylin-eosin, and the number of corpora lutea in the ovary and implants in the uterus were counted under a stereoscope.

Real-time RT-PCR analysis. Whole ovaries and corpora lutea were isolated from pregnant WT ($n = 12–16$) and *Mamld1* KO ($n = 12–18$) mice at 18.5 dpc, and uteri were isolated from four mice of each genotype at the same stage. Whole ovaries were also isolated from pregnant WT mice at 16.5 and 17.5 dpc ($n = 3$ and 5, respectively), pregnant KO mice at 20.5 dpc ($n = 5$), and WT mice at 0 or 1 day postpartum ($n = 4$). Tissues were immediately soaked in RNAlater solution (Life Technologies, Carlsbad, CA). Total RNA was extracted from homogenized samples by ISOGEN (Nippongene, Tokyo, Japan) and RNeasy Kit (QIAGEN, Valencia, CA). Contaminated genomic DNA was removed with a TURBO DNA-free kit (Life Technologies). cDNA was synthesized from 200 ng total RNA using a High Capacity cDNA Reverse Transcription kit (Life Technologies). We measured relative mRNA levels of genes implicated in the luteolytic process and/or regulation of *Akr1c18*. *Gapdh* was used as an internal control. The assays were performed using the ABI 7500 Fast real-time PCR system and TaqMan gene expression assay kit (Life Technologies). Primers and probes used in this study are listed in Supplementary Table S2.

***In situ* hybridization.** We examined *Mamld1* expression in the ovaries obtained from pregnant WT mice at 18.5 dpc. Paraffin sections were prepared as described above. *In situ* hybridization was performed using an antisense RNA probe for mouse *Mamld1*[18] (Genostaff Inc., Tokyo, Japan). The probe was digoxigenin-labeled using DIG RNA Labeling Mix (Roche, Basel, Switzerland). A sense cRNA for mouse *Mamld1* was used as a negative control. The colour of the probes was developed with NBT/BCIP solution (Sigma-Aldrich) and the sections were counterstained with Kernechtrot solution (Mutoh Chemical, Tokyo, Japan).

Western blot analysis. Tissue extracts were prepared from the ovaries of pregnant mice at 18.5 dpc and separated by standard SDS-PAGE (7.5% or 4–20% gradient gel; Bio-Rad, Hercules, CA). PVDF membranes were incubated in the solution containing the primary antibody. We used anti-20α-HSD antibodies (EB4002; KeraFAST Inc., Boston, MA), anti-NR4A1 antibodies (ab13851; Abcam, Cambridge, MA), and anti-STAT5B antibodies (ab178941; Abcam). Anti-ACTIN antibodies (A2066; Sigma-Aldrich) were used as an internal control. The signals were detected using Clarity Western ECL Substrate (Bio-Rad). All analyses were performed using three independent samples per group.

***In vitro* functional assays.** MLTC1 (CRL-2065™; ATCC, Manassas, VA) were maintained in RPMI 1640 medium containing 10% fetal bovine serum. For *Mamld1* knockdown assays, the cells were seeded in 6-well plates (1.0×10^5 cells/well) and transiently transfected with two siRNAs, i.e., siRNA1 (sense: 5′-CAGGAAUCGGGAACCAGUAAGAGAA-3′; and anti-sense: 5′-UUCUCUUACUGGUUCCCGAUUCCUG-3′) and siRNA2 (sense: 5′-CAGAGAUGC AGAUGCCCACAUUAAA-3′; and anti-sense: 5′-UUUAAUGUGGGCAUCUGCAUCUCUG-3′), or with a non-targeting control RNA (4611G; Life Technologies) (20 nM final concentration), using Lipofectamine RNAiMAX (Life Technologies). For *Mamld1* overexpression assays, the cells were seeded in 12-well plates (1.0×10^5 cells/well) and transfected with 200 ng of the expression vector of *Mamld1* or an empty expression vector (pCMV-Myc vector; Takara Bio, Otsu, Japan), using Lipofectamine 3000 (Life Technologies). The full-length *Mamld1* cDNA, which contains 2,412 nucleotides corresponding to the coding region without both 5′- and 3′-untranslated regions, was amplified from mouse fetal

testis-derived cDNA mixture (C57BL/6N; Sankyo Labo Service Corp. Inc.), and subcloned into a plasmid that was included in the TOPO TA cloning kit (Life Technologies). The cDNA that was missing the start codon was then subcloned into a pCMV-Myc vector to construct the *Mamld1* expression vector. The cells were harvested 24 hours after transfection. Total RNA were subjected to cDNA synthesis. Amounts of endogenous *Mamld1* and *Akr1c18* relative to that of *Gapdh* were analyzed by TaqMan real-time PCR in three independent experiments.

Statistical analysis. Data are expressed as the mean ± SEM. Statistical differences in mean values between two groups were examined by Student's *t*-test or Mann-Whitney's *U*-test, and differences in frequencies were examined by χ^2 test. *P* values less than 0.05 were considered significant.

References

1. Stocco, C., Telleria, C. & Gibori, G. The molecular control of corpus luteum formation, function, and regression. *Endocr. Rev.* **28,** 117–149 (2007).
2. Russell, J. A. & Leng, G. Sex, parturition and motherhood without oxytocin? *J. Endocrinol.* **157,** 343–359 (1998).
3. Zeng, Z., Velarde, M. C., Simmen, F. A. & Simmen, R. C. Delayed parturition and altered myometrial progesterone receptor isoform A expression in mice null for Kruppel-like factor 9. *Biol. Reprod.* **78,** 1029–1037 (2008).
4. Sfakianaki, A. K. & Norwitz, E. R. Mechanisms of progesterone action in inhibiting prematurity. *J. Matern. Fetal Neonatal Med.* **19,** 763–772 (2006).
5. Piekorz, R. P., Gingras, S., Hoffmeyer, A., Ihle, J. N. & Weinstein, Y. Regulation of progesterone levels during pregnancy and parturition by signal transducer and activator of transcription 5 and 20alpha-hydroxysteroid dehydrogenase. *Mol. Endocrinol.* **19,** 431–440 (2005).
6. Udy, G. B. *et al.* Requirement of STAT5b for sexual dimorphism of body growth rates and liver gene expression. *Proc. Natl Acad. Sci. USA* **94,** 7239–7244 (1997).
7. Teglund, S. *et al.* Stat5a and Stat5b proteins have essential and nonessential, or redundant, roles in cytokine responses. *Cell* **93,** 841–850 (1998).
8. Nio-Kobayashi, J. & Iwanaga, T. Differential cellular localization of galectin-1 and galectin-3 in the regressing corpus luteum of mice and their possible contribution to luteal cell elimination. *J. Histochem. Cytochem.* **58,** 741–749 (2010).
9. Stocco, C. O., Lau, L. F. & Gibori, G. A calcium/calmodulin-dependent activation of ERK1/2 mediates JunD phosphorylation and induction of nur77 and 20alpha-hsd genes by prostaglandin F2alpha in ovarian cells. *J. Biol. Chem.* **277,** 3293–3302 (2002).
10. Stocco, C. O. *et al.* Prostaglandin F2alpha-induced expression of 20alpha-hydroxysteroid dehydrogenase involves the transcription factor NUR77. *J. Biol. Chem.* **275,** 37202–37211 (2000).
11. Mejia, R., Waite, C. & Ascoli, M. Activation of Gq/11 in the mouse corpus luteum is required for parturition. *Mol. Endocrinol.* **29,** 238–246 (2015).
12. Sugimoto, Y. *et al.* Failure of parturition in mice lacking the prostaglandin F receptor. *Science* **277,** 681–683 (1997).
13. Sugimoto, Y., Inazumi, T. & Tsuchiya, S. Roles of prostaglandin receptors in female reproduction. *J. Biochem.* **157,** 73–80 (2015).
14. Foyouzi, N., Cai, Z., Sugimoto, Y. & Stocco, C. Changes in the expression of steroidogenic and antioxidant genes in the mouse corpus luteum during luteolysis. *Biol. Reprod.* **72,** 1134–1141 (2005).
15. Gross, G. A. *et al.* Opposing actions of prostaglandins and oxytocin determine the onset of murine labor. *Proc. Natl Acad. Sci. USA* **95,** 11875–11879 (1998).
16. Nio-Kobayashi, J. & Iwanaga, T. Galectin-1 and galectin-3 in the corpus luteum of mice are differentially regulated by prolactin and prostaglandin F2alpha. *Reproduction* **144,** 617–624 (2012).
17. Hernandez, F., Peluffo, M. C., Stouffer, R. L., Irusta, G. & Tesone, M. Role of the DLL4-NOTCH system in PGF2alpha-induced luteolysis in the pregnant rat. *Biol. Reprod.* **84,** 859–865 (2011).
18. Fukami, M. *et al.* CXorf6 is a causative gene for hypospadias. *Nat. Genet.* **38,** 1369–1371 (2006).
19. Kalfa, N. *et al.* Mutations of CXorf6 are associated with a range of severities of hypospadias. *Eur. J. Endocrinol.* **159,** 453–458 (2008).
20. Ogata, T., Laporte, J. & Fukami, M. MAMLD1 (CXorf6): a new gene involved in hypospadias. *Horm. Res.* **71,** 245–252 (2009).
21. Fukami, M. *et al.* Mastermind-like domain-containing 1 (MAMLD1 or CXorf6) transactivates the Hes3 promoter, augments testosterone production, and contains the SF1 target sequence. *J. Biol. Chem.* **283,** 5525–5532 (2008).
22. Nakamura, M. *et al. Mamld1* knockdown reduces testosterone production and *Cyp17a1* expression in mouse Leydig tumor cells. *PloS One* **6,** e19123 (2011).
23. Miyado, M. *et al. Mamld1* deficiency significantly reduces mRNA expression levels of multiple genes expressed in mouse fetal Leydig cells but permits normal genital and reproductive development. *Endocrinology* **153,** 6033–6040 (2012).
24. Uozumi, N. *et al.* Role of cytosolic phospholipase A2 in allergic response and parturition. *Nature* **390,** 618–622 (1997).
25. Mahendroo, M. S., Porter, A., Russell, D. W. & Word, R. A. The parturition defect in steroid 5alpha-reductase type 1 knockout mice is due to impaired cervical ripening. *Mol. Endocrinol.* **13,** 981–992 (1999).
26. Timmons, B. C. & Mahendroo, M. S. Timing of neutrophil activation and expression of proinflammatory markers do not support a role for neutrophils in cervical ripening in the mouse. *Biol. Reprod.* **74,** 236–245 (2006).
27. Soldin, S. J. & Soldin, O. P. Steroid hormone analysis by tandem mass spectrometry. *Clin. Chem.* **55,** 1061–1066 (2009).
28. Devi, Y. S. & Halperin, J. Reproductive actions of prolactin mediated through short and long receptor isoforms. *Mol. Cell Endocrinol.* **382,** 400–410 (2014).
29. Curlewis, J. D. *et al.* A prostaglandin f(2alpha) analog induces suppressors of cytokine signaling-3 expression in the corpus luteum of the pregnant rat: a potential new mechanism in luteolysis. *Endocrinology* **143,** 3984–3993 (2002).
30. Imamura, T., Luedke, C. E., Vogt, S. K. & Muglia, L. J. Oxytocin modulates the onset of murine parturition by competing ovarian and uterine effects. *Am. J. Physiol. Regul. Integr. Comp. Physiol.* **279,** R1061–R1067 (2000).

Acknowledgments

We thank Ms. Emma L. Barber (National Center for Child Health and Development, Tokyo, Japan) for editing this manuscript. This work was supported by the following grants: the Grant-in-Aid for Young Scientists (B) (grant number 26870887 to M.M.) from the Japan Society for the Promotion of Science; the Grant-in-Aid for Scientific Research on Innovative Areas from the Ministry of Education, Culture, Sports, Science and Technology; the Grant for Research on Intractable Diseases from the Ministry of Health, Labour and Welfare; and grants from the National Center for Child Health and Development